

HYBRID TECHNOLOGY COMBINING ELECTRON BEAM WELDING AND FRICTION STIR WELDING IN THE PROCESSES OF REPAIR OF AIRCRAFT STRUCTURE ELEMENTS OF MAGNESIUM ALLOYS

A.L. MAJSTRENKO¹, V.M. NESTERENKOV², R.V. STRASHKO², S.D. ZABOLOTNY¹ and V.N. TKACH¹

¹V.N. Bakul Institute for Superhard Materials, NASU

2 Avtozavodskaya Str., 04074, Kiev, Ukraine. E-mail:alcon@ism.kiev.ua

²E.O. Paton Electric Welding Institute, NASU

11 Kazimir Malevich Str., 03680, Kiev, Ukraine. E-mail: office@paton.kiev.ua

A technological process is developed for friction stir processing of surface layers of the parts from magnesium and aluminum alloys for the purpose of their modifying aimed at formation of a layer of fine-grain structure (of 1.2–4.5 μm) that is 16–63 times lower a grain size of base metal (75.8 μm). Formation of microcracks is shown at the interface of EB-weld metal and base metal of magnesium alloy ML10 as well as their absence in welding through intermediate zone with FS-modified fine-grain structure. It provided for the possibility of increase of strength of EB-welded joints from ML10 alloy. 8 Ref., 1 Table, 13 Figures.

Keywords: *electron beam welding, friction stir welding, modified fine-grain structure, microstructure grain size*

Magnesium alloys are particularly important in aircraft and space engineering due to the fact that they differ by relatively high strength at low specific weight [1–4]. Structural magnesium alloys are divided on wrought and cast ones. The main alloying elements in the cast alloys are aluminum, zinc, manganese, silicon, cerium, zirconium and thorium. However, at all positive characteristics and properties these alloys refer to difficult-to-weld materials. These difficulties are caused, first of all, by formation of defect of pore and cavity type in the welds due to appearance in a zone of electric arc effect the local temperatures exceeding not only zinc melting temperature (419.5 °C), but its evaporation temperature (907 °C). Therefore, all the investigations aimed at producing solid, homogeneous and strong welded joint of the parts from wrought and cast magnesium alloys are still relevant. One of the most perspective method in this case is vacuum EBW.

The investigations on vacuum weldability of magnesium alloys ML using electron beam were carried out on UL-209M unit with computer regulation of all parameters and systems [5] developed at PWI (Figure 1). The unit is equipped with power complex based on ELA-60/60 and EB gun moving inside the vacuum chamber along X , Y , Z linear coordinates as well as turning about the axis Y – Y in coordinate QC through 0–90° angle. Air from vacuum chamber of internal dimension 3850×2500×2500 mm and volume 24.1 m³ is pumped in automatic mode to working

vacuum $2.66 \cdot 10^{-2}$ Pa for less than 30 min. At $U_{acc} = 60$ kV the EB gun with tungsten cathode together with power complex ELA-60/60 provides for electron beam current range $I_b = 0$ –500 mA as well as performance of different technological beam scan in process of EBW. An accuracy of EB gun positioning in the coordinates is not less than 0.1 mm. An image of welding place is visualized in the secondary emission electrons, and combining of electron beam with butt is provided by RASTR system with the accuracy not worth than 0.1 mm [6].

Formation of a keyhole in molten metal is caused by the following factors, namely material evaporation, displacement of liquid metal by pressure of beam electrons, displacement of liquid metal by evaporation



Figure 1. UL-209M unit for vacuum EBW

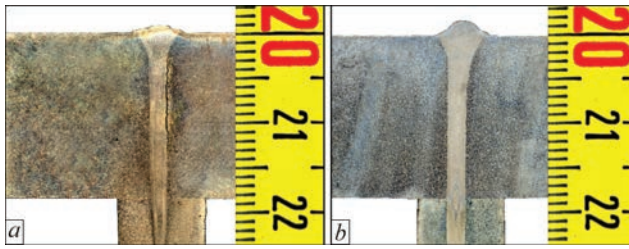


Figure 2. Macrostructure of welded joint of magnesium alloy ML10 of 18.5 mm thickness in downhand EBW with run-on plate without preliminary FSP (a) and with FSP (b)

recoil pressure, surface tension force and hydrostatic pressure of liquid metal. Molten metal pressure has significant impact on the weld and defect formation. This pressure is in particular obvious in welding of metals of 20 mm thickness. In this connection, task solution for welding of medium and large thickness metals required a change of position of electron beam and weld pool to horizontal one. It provided for more favorable conditions of liquid metal transfer in a crater. Horizontal positioning of a pool also facilitates liquid metal degassing and its refining.

Welding of cast magnesium alloy ML10 of $\delta = 6$ mm was also carried out by vertical welds without run-on plate using horizontal electron beam on upward and downward schemes. The specimens of $150 \times 100 \times 6$ mm size were subjected to preliminary friction stir processing (FSP). Analysis of carried experiments showed that the vertical welds produced with horizontal electron beam have satisfactory formation using both schemes. Figure 2 shows that width of the weld rises in a root part according to both schemes at increase of welding current at $v_w = 20$ mm/s, refocusing $+ \Delta I_f = 30$ mA, diameter of circular technological scan of electron beam $d_{cir} = 1$ mm and working distance $l_{work} = 200$ mm. No defects in form of undercuts, depressions and cracks were found along the fusion line and in HAZ.

Since the weld metal dendrites start growing from the base metal grains on fusion line, the size of crys-

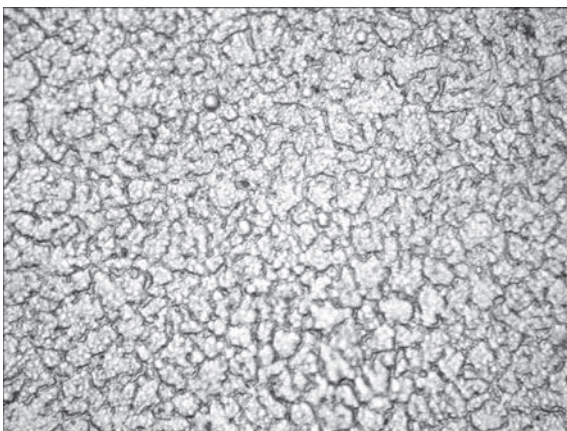


Figure 3. Microstructure ($\times 1000$) of weld of magnesium alloy ML10 made with EBW

tallites depends on these grain dimensions. Chemical inhomogeneity has negative effect on the final physical-chemical properties of welded joints, and during weld pool solidification promotes for formation of the weld defects. i.e. solidification cracks. Increase of solidification rate and, respectively, reduction of size of dendrites and inter-dendrite areas can be referred to the main measures, aimed at elimination of microchemical inhomogeneity. Therefore, preliminary refinements of the base metal grains promotes for certain decrease of size of weld crystallites. It is well known fact that HAZ in non-ferrous metal and alloys, including magnesium ones, consists of structural areas similar to areas in steel, i.e. area of partial melting — narrow transition band from weld metal to base metal, including submelted and solidified grains of the base metal. The weld crystallites coalesce with the coarse grains of base metal in this solid-liquid state area. A liquation of additives is possible in this case, therefore, this area has significant effect on welded joint quality. Formation of the liquid interlayers at grain boundaries results in reduction of the mechanical properties of welded joints and, quite often, crack appearance.

A fractographic examination of specimen fracture surfaces carried out on «Neophot-32» and «Versamet» microscopes showed that the metal fracture, reflecting overheating condition in the weld to base metal fusion zone, takes place parallel to the axis of applied load. Thickening of grain boundaries takes place in the weld zone structure in arc methods of welding as well as presence of triple compounds and significant amount of eutectics can be observed. In contrast to mentioned above, EBW promotes for mainly polyhedral structure and formation of eutectic reduces, that has positive effect on metal hardness level.

The weld has a fine-disperse, cast structure consisting of α -solid solution of complex composition and uniformly distributed phase precipitates, apparently, Mg_4Al_3 (Figure 3). Besides, presence of round precipitates of light colour (Figure 4) should be noted. Weld hardness reaches $HV01-658-782$ MPa.

Amount of fine grains in the structure increases in withdrawal from the fusion line, the structural constituents remain the same. The structure of base metal consists of alternating bands of different size grains (Figure 5). Lower amount of inclusions and non-dissolved phase (probably Mg_4Al_3) is noted in the structure in comparison with HAZ structure. Hardness at specimen edge makes $HV01-762-772$ MPa.

Hybrid FSW + EBW technology. EBW in comparison with known methods of fusion welding is characterized by high specific concentration of energy, ideal conditions of vacuum shield of molten metal,

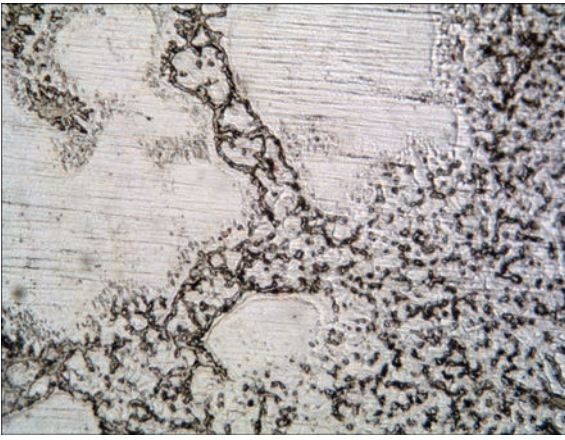


Figure 4. Microstructure ($\times 500$) of ML10 alloy along the fusion line in EBW

high welding speed, low values of energy input rate, small width of HAZ, narrow penetration zone and small volume of weld liquid-phase pool, insignificant heat deformations of parts being welded, high flexibility and large range of process capabilities. This sets it apart from other fusion arc welding methods. Nevertheless, fusion welding of magnesium alloys provokes for structural transformations in the weld metal and near-weld zone. Such areas acquire different mechanical properties, due to what a welded joint strength in comparison with a base metal is reduced in some cases to 50–60 %, and formation of cracks (Figure 6) is observed along the fusion line and in the near-weld zones.

Therefore, it is relevant to develop a hybrid technology, which would join high technological effectiveness of EBW and possibility of production of high-strength joints using FSW in order to apply it during manufacture and renewal of life of structures of aircraft and space engineering from aluminum and magnesium alloys. The received process capabilities were also used for modifying a structure of cast magnesium alloy ML10 due to effect of friction stir process on change of a structure of parts' surface layer, which are thereupon being welded using EBW. The idea of structure modifying lied in purposeful refinement of grain size in the processed layer of base metal to 6–8 mm depth.

Influence of preliminary FSP of surface layers of welded parts. FSW proposed in 1991 by TWI [7] refers to the methods of solid-phase joining and differs from traditional friction welding methods. The tool with small diameter pin and shoulder (Figures 7 and 8) pressed in metal being welded at rotation and generating heat emission due to friction work between the tool surfaces and metal being welded, and work of plastic deformations. This results in metal local heating to temperature sufficient for reduction of its hardness and plasticization to ductile-plastic state, after what the tool starts proceed-

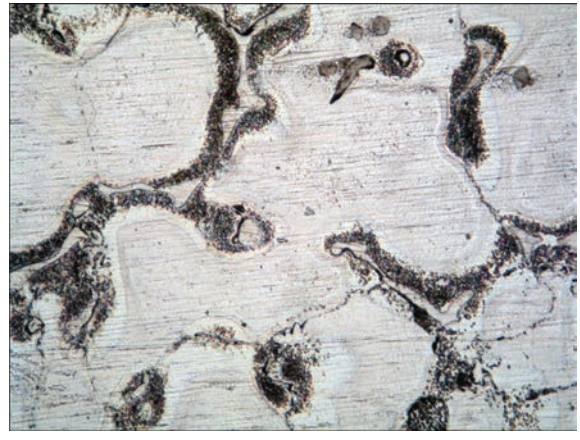


Figure 5. Microstructure ($\times 500$) of base ML10 metal

ing along parts' interface, provoking plastic stirring of metal of adjacent surface layers in mating parts, by this forming a permanent joint. Thus, formation of the welded joint took place at temperatures significantly lower than in liquid-phase fusion welding, that has vital effect on the structure of formed weld and its strength, but also minimizes residual stresses in HAZ and temperature deformations. It is very attractive for aircraft and automotive industry. Currently, these branches realize number of examples of FSW of metals of 1–10 mm thickness.

It is well know fact that FSW has a number of advantages in comparison with fusion welding. In particular, there is a possibility of joint formation in solid phase, high efficiency and quality (absence of porosity, inclusions, cavities), wide range of welded similar and dissimilar metals with different physical-chemi-

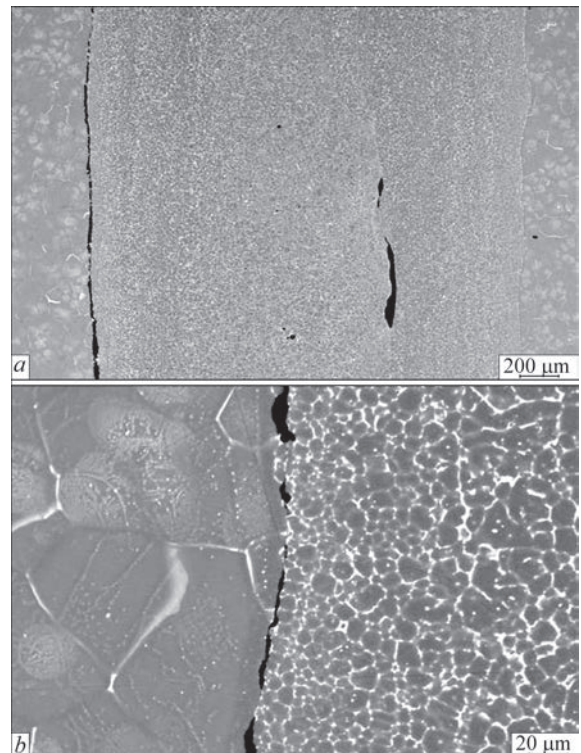


Figure 6. Delamination of weld metal from base metal in EB-welded specimen of magnesium alloy ML10

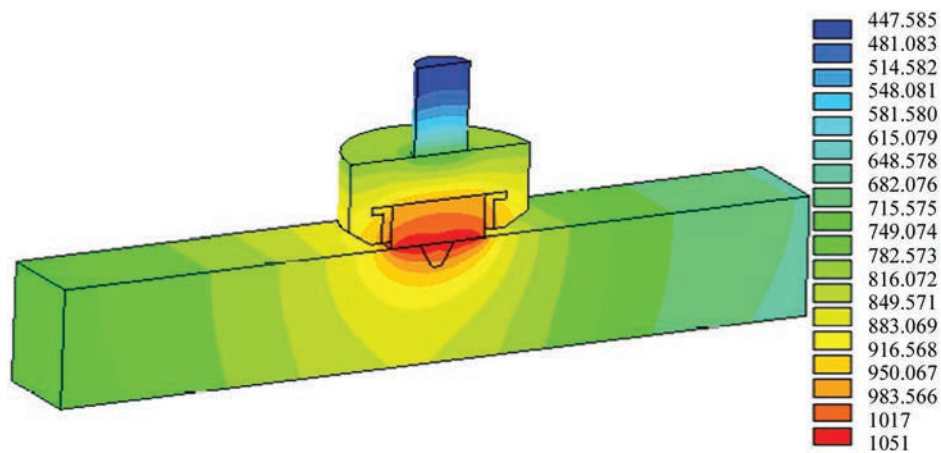


Figure 7. Scheme of FSW

cal properties, absence of auxiliary welding consumables and possibility of performance of operations in any spatial positions.

As it was shown in work [8] FSW provokes for transformation of initial coarse-grain structure of the base metal into fine-grain one in the stir zone. Besides, crystalline particles, formed in the processes of primary solidification (after alloy casting), are fractured in the surface layers of metals being welded, rolling-oriented grains are eliminated and their size is significantly reduced (Figure 9).

Hybrid FSW + EBW technology was tested in welding of magnesium alloy ML10 of 20 mm thickness using downhand scheme with vertical electron beam and run-on plate from the same alloy. The surface layers of specimens were preliminary FS-pro-

cessed on vertical knee-and-column type milling machine of 6L12P model to 6 mm depth at tool rotation rate 800 rpm and linear rate of tool movement 31.5 mm/min. After FSP the surfaces of edges to be welded were milled. EBW of butt specimens was carried out in a special device from non-magnetic materials. Penetration geometry of the formed welded joints differ by fusion walls virtually parallel base metal on depth. Carried investigations on ML alloys 5–30 mm thick mastering of hybrid welding technology showed welded joints' stable formation.

Thus, it is determined that hybrid welding by vertical electron beam in downhand position and horizontal electron beam using vertical upward and downward schemes provided for satisfactory formation of the welded joints and elimination of defects of ML alloys at through penetration of specimens to $\delta \leq 10$ mm even without use of the run-on plates. There is a necessity in application of the run-on plates in welding of ML alloy specimens of $\delta > 10$ mm due to formation of undercuts and depressions in a weld root part, which take place in all considered schemes at through penetration.

Metallographic examinations of ML10 alloy welded joints were divided in the following way. A hybrid-welded joint is located on the first specimen. Such a sequence (FSW + EBW) of metal effecting assumes preliminary change of the initial structure of surface layers of alloy subjected to FSP with their further EBW. A welded joint made using simple EBW without FSW application was performed on the second specimen. A structure was developed by means of chemical etching in 10 % aqueous solution of citric acid.

A microstructure of weld in examined specimens represent itself a mixture of δ -phase (solution based on magnesium) and intermetallics (see Figures 4 and 5). The weld structure is cast and fine dispersed, weld metal hardness of specimen 1 was HV05-779–



Figure 8. View of tool made from steel P18 (a), and FSP of surface layer of ML10 alloy block (b)

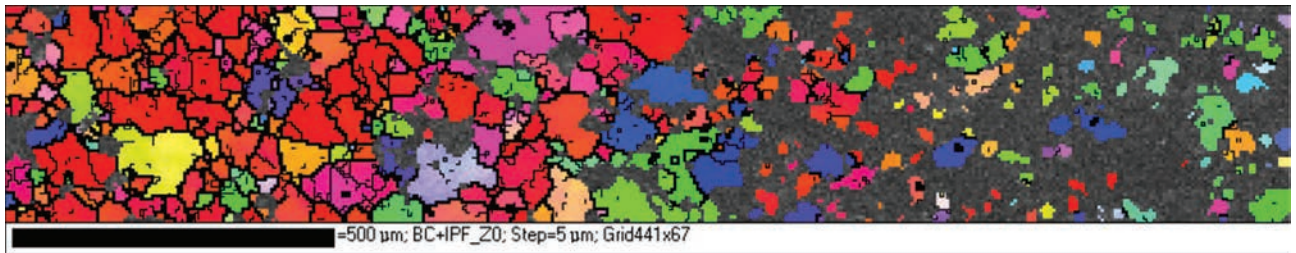


Figure 9. Backscattered electron diffraction image of microstructure of ML10 alloy at interface of initial metal and modified layer after FSP to 6 mm depth

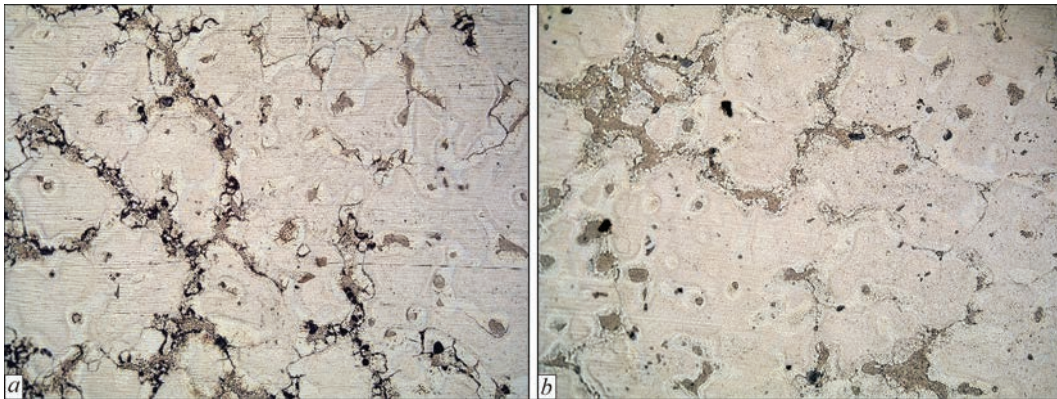


Figure 10. Microstructure ($\times 200$) of HAZ areas of hybrid-welded specimens 1 (a) and 2 (b)

906 MPa and that of specimen 2 $HV05-826-934$ MPa. The microstructure of weld metal of investigated specimens included the different shape particles (see Figure 4). The precipitates of the same type are present in HAZ (Figure 10) and base metal of examined specimens (see Figures 4 and 5). The structures of weld metal of specimens 1 and 2 differ by somewhat coarser size of the structural constituents in specimen 2 in comparison with specimen 1. The structure of HAZ metal in specimens 1 and 2 represent itself coarse grains of solid solution of alloying elements in magnesium. Compressing them harder eutectic mixture of solid solution (δ -solution) and intermetallic compound are located along the grain boundaries, and it should be noted that the eutectic mixture continues weld structure (see Figure 4). Eutectic amount is reduced in a direction from the fusion line, and eutectic mixture is located only by small fragments along the grain boundaries of δ -solid solution at 500 (specimen 1) and 700 μm distance (specimen 2). HAZ extension in specimen 1 reached 1200 μm and that in specimen 2 was 1500 μm .

A microstructure of base metal (see Figure 5) consists of grains of δ -solid solution (hardness $HV01-612-665$ MPa), eutectic ($HV01-946$ MPa) is precipitated along the boundaries and light phase with $HV01-1400$ and 1330 MPa is precipitated in the center of eutectic. Hardness of grains of δ -solid solution close to eutectic reaches $HV01-707$ MPa.

Mechanical properties of EB-welded joints. The mechanical tests were carried out for testing a qual-

ity of welded joints of magnesium alloy ML10. The results of pulling tests allow determining the other parameters of welded joint strength, i.e. $\sigma_{0.2}$, δ and ψ (see the Table), in addition to σ_t value. The specimens of welded joints were tested in as-delivered condition, after EBW as well as after hybrid FSW + EBW. The pulling tests of welded joints were carried out using cylinder specimens of 3 mm test portion diameter.

As it follows from Figure 11, failure of specimens after EBW takes place mainly along the fusion line and HAZ, and after FSW + EBW it takes place in a distance from the weld and out of the HAZ (Figure 12). Ductility of the welded joints (δ , ψ) rises insignificantly in comparison with ductility of the base metal, and toughness a_n increases by 30 % and more. Strength of the hybrid-welded joints, increases in comparison with welded joint strength produced without FSP, and reaches $\sigma_{t\text{wj}}/\sigma_{t\text{bm}} = 94\%$.

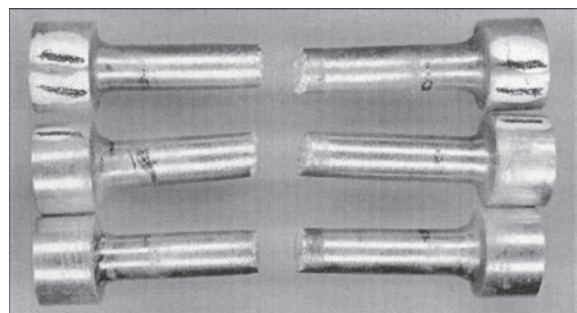


Figure 11. EB-welded specimens of magnesium alloy ML10 after mechanical pulling tests

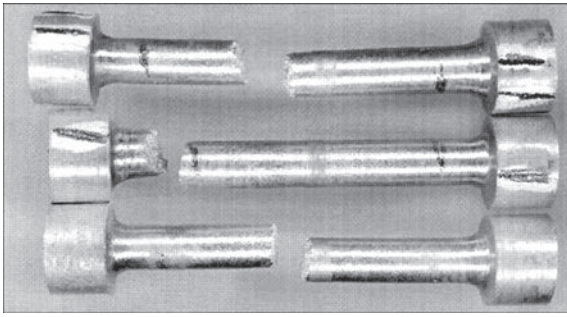


Figure 12. View of specimens of magnesium alloy ML10 with FS-modified structure of alloy layers adjacent to butt and then EB-welded at $U_{acc} = 60$ kV, $I_b = 50$ mA, $v_{EBW} = 20$ mm/s, $\Delta I_f = 5$ mA and $I_{work} = 200$ mm after uniaxial tension tests

It should be noted that formation of cracks (see Figure 6) is observed after EBW at the interface of weld metal recrystallization zone through liquid phase and base ML10 metal. This phenomenon is considered in more details and approximate evaluation of the reasons of its formation will be carried out.

It is known fact that the volumetric compression modulus of magnesium alloy ML10 equals 41.2 GPa, coefficient of thermal expansion $\alpha = 0.0000225$ K⁻¹ at room temperature and $\alpha = 0.000102$ K⁻¹ [3, 4] at liquid phase temperature 650 °C, i.e. their ratio reaches 4.53. Thus, we can evaluate the value of temperature stresses, which appear in the weld metal produced by EBW, due to thermoelastic variance to the characteristics of base ML10 metal at cooling after welding from liquid phase temperature (650 °C) to room temperature, i.e. $\sigma_{ts} \approx K\Delta\alpha\Delta T \approx 41200 \cdot 0.00008 \cdot 600 = 1997$ MPa. Formed thermal stresses reach 2 GPa level and tensile ultimate strength of this alloy (at room temperature) equals only $\sigma_t = 226$ MPa. Therefore, it is obvious that formation of microcracks along the interface of these zones is caused by effect of supercritical tensile stresses. Apparently, that reduction of strength of the EB-welded ML10 alloy joint is caused by appearance of microcracks along the weld body to base metal interface (see Figure 6). Thus, it can be concluded that the proposed hybrid technology (FSW + EBW) allows significant change of the situation in comparison with traditional EBW by increase of the strength characteristics of magnesium alloy welded joint at that preserving its ductility (see the Table). In this connection, it is proposed to carry out preliminary change of base metal structure, i.e. its modification, before EBW. It lies in directed refinement of metal grains in surface layers of the parts being welded.

Mechanical properties of welded joints of magnesium alloy ML10

Specimen type	σ_t , MPa	$\sigma_{0.2}$, MPa	δ , %	ψ , %
Base metal	230.6	140.0	5.9	11.1
EB-welded joint	197.9	134.3	6.5	12.0
After EBW of parts with FS-modified surface layers	216.8	153.9	6.6	12.5

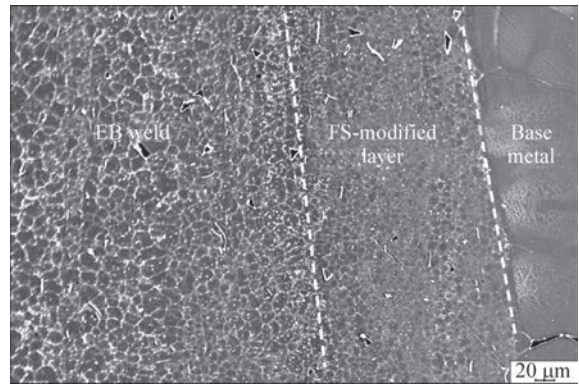


Figure 13. View of joint structure of parts from ML10 alloy with preliminary modified surface layers ($v_{FSW} = 31.5$ mm/min; $\omega = 800$ rpm) and further EBW (dashed lines — conditional EB-weld, FSP-weld and base metal interfaces)

As it was mentioned above, essence of the process of structure modification during FSW lies in grain refinement of the processed layer to 6–8 mm depth in comparison with the base metal [6] (see Figures 6 and 9). Such a refinement by Hall–Petch law can result in increase of metal strength in this zone. Besides, a conclusion on state of crystallites in the FSW and EBW deformed zones can be done based on analysis of image in Figure 9.

Thus, fracture and disorientation of crystallites of the initial metal can be observed in the FSP zone using a method of backscattered electrons on ZEISS EVO SEM, equipped with energy-dispersion analyzer INCA PENTA Fetx3. It results in formation of fine-grain alloy structure (grain size 1.2–4.5 μm), that is 16–63 times less the grain size (75.8 μm) in the initial metal. At that it should be noted that initial orientation of the crystallines (in the base metal) in the modified layer is completely disoriented (see Figure 9).

Change of parameters of the structure of ML10 alloy modified specimens depends on parameters of tool movement (tool rotation rate and speed of welding). SEM-images of grain boundaries of mating modified layer and base ML10 metal (see Figure 9) indicate high level of effect of modification process on change of alloy structure state in form of significant refinement of base metal grains.

Exactly this peculiarity of structure change of ML10 alloy, received as a result of preliminary FS modification of the surface layer (to 6 mm depth), was used for further joining the parts by vacuum EBW for the purpose of increase of weld strength. Figure 13 shows the structure of ML10 alloy, received as a result

of EBW its parts after preliminary FSP of the surface layers. At the same time, formation of an intermediate structured fine-grain area, having no observable hot cracks (see Figure 6), is noted after EBW between recrystallization zone and base metal. The fractographic examination of structure state of the welded joint with modified layer (after FSP to 6 mm depth) showed that the preliminary processing of the surface layers of part edges results in the fact that further EB joining takes place already not over the alloy in the initial state with 75.8 μm grain size (see Figure 13), but on metal with FS-formed fine-grain structure of 1–4 μm size. Moreover, in the zone of weld metal recrystallization through liquid phase the alloy grain size increases only to 9.3–9.8 μm , that is 1.5 times more the size of grain in FS processing zone, but 7–8 times less than in the base metal.

But the most important lies in formation of the intermediate fine-grain area (grain size 6.4 μm), in which microcracks are already observed (see Figure 13), between the recrystallization zone and base metal. This Figure shows the structure state of ML10 alloy in the modified layer as well as conditional interfaces of layers after FSP.

The experiments show that the temperature in processing zone does not exceed $(0.5-0.7)T_m$ but melting temperature of magnesium alloys is in the range from 650 to 680 $^{\circ}\text{C}$, i.e. temperature in the zone of tool with metal interaction in the process of its structure modification is possible in 270–320 $^{\circ}\text{C}$ limits [8]. The temperature in FSP zone was measured using digital contact-free infrared thermometer DT-8833. Mechanical pulling tests of welded joints of ML10 alloys showed (see the Table) that fracture after EBW with preliminary FSP takes place mainly out of the HAZ (see Figure 12).

Conclusions

1. The optimum modes were determined for EBW of ML magnesium alloy 5–30 mm thick providing set penetration geometry in different spatial positions.

2. Formation of the microcracks at a mating interface of recrystallization zone through weld metal liquid phase and ML10 base metal in EBW as well as their absence in welding through intermediate zone

with FS-modified fine-grain structure is shown for the first time.

3. The tools were developed for preliminary FSP of the surface layers of edges of plates of cast magnesium alloy ML10 for modification of their structure, directed on formation of alloy fine-grain structure (grain size 1.2–4.5 μm) which 16–63 times less the size of initial grains (75.8 μm).

4. Metallographic examinations of alloy ML welded joints were carried out, which verified formation of finer structural constituents in the case of FSP application.

5. For the first time it is determined that in EBW over modified layers of specimens of ML10 alloy the zone of FS-modified fine-grain structure with grain size 11.8 times less than that in the initial one, i.e. 6.4 μm , is formed. It lies between the recrystallization zone through liquid phase of weld metal, made by EBW, with alloy grain size 7–8 times less than that of the base metal (75.8 μm), i.e. 9.3–9.8 μm . In addition, for the first time it was found that the average size of grains increases to 6.4 μm from metal recrystallization zone to EBW zone in FS-modified layer (grain size 1.2–4.5 μm) during its heating and cooling.

6. The technology was developed for hybrid FSW + EBW welding of magnesium alloys MA and ML of up to 30 mm thickness which allows eliminating crack formation and increasing strength characteristics of the welded joints.

1. GOST 14957–76: Magnesium wrought alloys. Grades.
2. GOST 2856–79: Magnesium cast alloys. Grades.
3. Krymov, V.V. (1960) Magnesium cast alloys and their application in engineering. In: *Magnesium alloys*. Moscow.
4. Portnoj, K.I., Lebedev, A.A. (1952) *Magnesium alloys*: Refer. Book. Moscow.
5. Nazarenko, O.K., Nesterenkov, V.M., Neporozhny, Yu.V. (2001) Design and electron beam welding of vacuum chambers. *The Paton Welding J.*, **6**, 40–42.
6. Paton, B.E., Nazarenko, O.K., Nesterenkov, V.M. et al. (2004) Computer control of electron beam welding with multi-coordinate displacements of the gun and workpiece. *Ibid.*, **5**, 2–5.
7. Thomas, W.M., Nicholas, E.D., Needham, J.C. et al. *Friction stir butt welding*. Int. pat. appl. PCT/GB92/02203; GB pat. appl. 9125978.8; US pat. appl. 5,460,317. Publ. Dec. 1991.
8. *Report on R&D*: Development of tools from superhard materials for friction stir welding designed for producing and restoration of structures of aeronautical and space engineering from aluminium and magnesium alloys in the frame of program RES URS R 8.6.1. Kyiv: INM.

Received 11.04.2016